J. Mater. Environ. Sci. 7 (8) (2016) 2739-2747
ISSN : 2028-2508
CODEN: JMESCN

Mortar's design from shell powders associated with LDH nanocomposite Ti - Zn -type

F. Amor [1]*, A. Diouri [1]*, S. Kamali-Bernard [2]

[1]: Laboratoire de Chimie du Solide Appliquée, Faculté des Sciences, Université Mohammed V-Agdal, B.P. 1014. R.P.- Avenue Ibn Battouta, 10000 Rabat, Maroc.

[2]: Laboratoire de Génie Civil et Génie Mécanique, INSA de Rennes, 20 Av.des Buttes de Coësmes, 35043 Rennes Cedex France.

Received 13 Oct 2015, Revised 12 May 2016, Accepted 16 May 2016
**Corresponding author. E-mail: amorfouad@gmail.com, abdeljebbar.diouri@gmail.com;*

Abstract

The active photo-catalytic TiO_2 has been widely applied in the science of building materials because of its ability to remove pollutants from surface of buildings. This approach can be beneficial for the design of building materials to reduce environmental impact. Actually, new inorganic nanocomposites based layered double hydroxides (LDH) associated with TiO_2 are introduced to increase the compatibility of the photocatalyst with the mortar. In this paper, we introduce other nanocomposites LDH associated with zinc, as additions to the Portland cement mortars; the aim is to study the physico-chemical properties of the elaborated mortars. The permeability and mechanical properties of mixtures based on mineral powders of small particle size of shell powders associated with LDH nanocomposites type Ti-Zn are tested. Measurements of apparent density, porosity to water and permeability, mechanical properties and Scanning Electron Microscopy were performed. The results show that these properties are similar to those of standardized mortars.

Keywords: active photo-catalytic TiO_2, pollutants, nanocomposites, layered double hydroxides.

1. Introduction

In recent years, the increasing interest in the combination of active materials with photocatalytic cementitious materials has been recognized in several produced publications [1-5]. Most published studies refer to the application of nano-powders based on TiO_2 like active photocatalytic material [2,6,7,8], the influence of moderate additions of titanium oxide is considered as one of mineralizers, the presence of a small amount (<5%) TiO_2 apparently increases the hydraulic activity of cement [9]. Several researchers introduced the TiO_2 in cementitious materials as a photocatalyst for the degradation of gaseous pollutants (NO_x) [10]. The titanium oxide on the surfaces of urban buildings can trap volatile molecules. Using the UV photocatalytic reaction, these materials degrade some toxic molecules, and in the presence of rain, urban surfaces are washed. The use of mineral TiO_2 powders was also the basis of development of durability and aesthetics properties in mortars based Portland cement. Titanium oxide is the most widely used white pigment; it is not toxic and obtained from the titanium ore. Approximately 95% of the amount of extracted ore is used for producing the pigment, and only 5% for the preparation of metal. It is thus very inert chemically. It is insoluble in all fluids except concentrated sulfuric acid and hydrofluoric acid [11]. Among some photocatalyst, TiO_2 is the most popular material due to its high band gap energy (3.2eV) and less toxicity. Degradation of hazardous substances by TiO_2 is assigned to reduction-oxidation reactions generated from absorption of photons by TiO_2 that leads to a photoexication: formation of electron–positive hole pairs [28]. Zhang and Li [12] have reported that the addition of nano-

particles refines the structure of concrete pores and improves the resistance to the penetration of chlorides in concrete. The affinity of the pore structure and the resistance of the concrete to chlorides penetration are increased with the presence of nano-particles. Since the seventies the layered double hydroxides (LDH) are the subject of increasing interest for their anion exchange properties, and their magnetic properties and their electrochemical use in heterogeneous catalysis. These materials are composed of positively charged sheets containing divalent and trivalent cations. The electro-neutrality of the material is ensured by the presence of interlayer anions, solvated by water molecules. They have an exceptionally flexible composition, which gives them exchange properties, intercalation, conduction etc. ..., opening onto vast areas of applications such as environmental catalysis [13, 14].

LDHs associated with zinc, used as additions to cement, in a mortar, improve photocatalytic reactivity and hydraulic properties for mortars more efficient self-cleaning. Zinc is selected as an addition to LDH because of its photocatalytic activity with the intention of contributing to the overall activity of the new nanocomposite Ti-Zn [15]. ZnO is frequently looked as an alternative to TiO_2, since it can absorb a larger energy fraction of the solar spectrum and more light quanta [29].

Studies on the solidification of nickel chloride in cement prepared with a water cement ratio, W / C = 0.65 showed an accelerating effect on the physical characteristics of the matrix and a better value of the compressive strength of 21 MPa. Nickel leaching results have a very low constant concentration in a leaching medium with ph=12.5, indicating a good retention capacity of the cement matrix [16].

Studies of oyster shells, used as mineral adjuvant to optimize geopolymer cement properties obtained from volcanic slag, showed that the major mineral of oyster shells is the calcite used to compensate the deficit CaO in volcanic slag. This mineral addition has reduced the initial setting time and improved the compressive strength [17]. The oyster shells are marine waste that can be valorized in the construction sector. It is noted that the oyster shell powders consist entirely of calcium carbonate with few impurities [30, 31]. When these powders are introduced in the concrete, workability decreases with the degree of substitution. It is found that the addition of OS powders does not cause a decrease in the compressive strength of concrete at the age of 28 days [32].

The objective of this experimental study is to evaluate the behavior of layered double hydroxides associated with the TiO_2, zinc and shell powder in a cementitious mortars. The choice of the valuation track fell on the hydraulic binder due to the similarity in chemical composition between the shell powder and limestone. This choice is an ideal solution to respond to the two requirements that are the management of oyster shells as waste in the borders of the beaches and the reduction of resource consumption. The experimental study was carried out on mortars. The conducted research is to study the hydraulic and mechanical behavior of the mixtures elaborated from Portland cement, sand, shell powder, TiO_2 powder and low granulometry LDH powder containing zinc. Measurements of apparent density, porosity to water and permeability, mechanical properties and Scanning Electron Microscopy will be performed in comparison with those of standardized mortars.

2. Materials and methods

2.1. Materials and mixtures formulation

The sample mortars used are confectioned from: Portland cement CEM I 52.5, standard sand, shell powder (from Morbihan northwest of France), TiO_2 powder and added LDH powders synthesized in the form: LDH-TiO_2-Zn; this powder is synthesized by the wet impregnation method of TiO_2 on layered double hydroxides (LDH)-Zn which was used for the preparation of nanocomposites LDH-Ti-Zn. Before the impregnation process, the LDH-Zn are synthesized by the method of low supersaturation (LS) according to co-precipitation method at constant pH. Precursor Zn (NO_3) $26H_2O$ is added in a continuous manner at a constant temperature with the simultaneous addition of Na_2CO_3 and NaOH. The wet impregnation process was carried out using the TiO_2 powder that was diluted (3 mass %) in a 0.67 M Na_2CO_3 base solution and added onto Zn-LDH powder. The sample was dried for 12 hours at 100°C and calcined for 5 hours at 500 °C.

The formulation used for the calculation of the porosity accessible to water, density, permeability, resistance to compression and flexural is described in Table 1.

Table 1: Formulation of the samples based shell powder and LDH (Weight %).

Mortars	Cement 52.5	Sand	water	Shell powder	TiO_2	LDH-TiO_2-Zn
CS	22.2	66.7	11.1	0	0	0
CSO5	17.2	66.7	11.1	5	0	0
CSO5T1	16.2	66.7	11.1	5	1	0
CSO5TLZ1	16.2	66.7	11.1	5	0	1
CSO5TLZ3	14.2	66.7	11.1	5	0	3
CSO10	12.2	66.7	11.1	10	0	0
CSO10T1	11.2	66.7	11.1	10	1	0
CSO10TLZ1	11.2	66.7	11.1	10	0	1
CSO10TLZ3	9.2	66.7	11.1	10	0	3

2.2. Apparent density and porosity accessible to water

The apparent density and the porosity accessible to water were determined on cylindrical specimens of 40 mm diameter and 80 mm height. The test protocol is consistent with the recommendations of AFREM group [18]. The samples were first kept under vacuum for 24 hours in a vacuum bell, they were then immersed in water and maintained under vacuum for 48h. Determining the sample volume was then performed by weighing in air and in water with a hydrostatic weighing device. For the dry mass, the samples were dried at (105 ± 5)°C until constant weight. The porosity accessible to water is finally expressed as volumetric percentage.

2.3. Permeability

We chose to measure the permeability of the studied mortars using a constant head permeameter. The principle is to maintain a difference of constant gas pressure between two extremities of the sample, and measuring the resulting flow when the steady state is established. The experimental setup is shown in the figure 1.

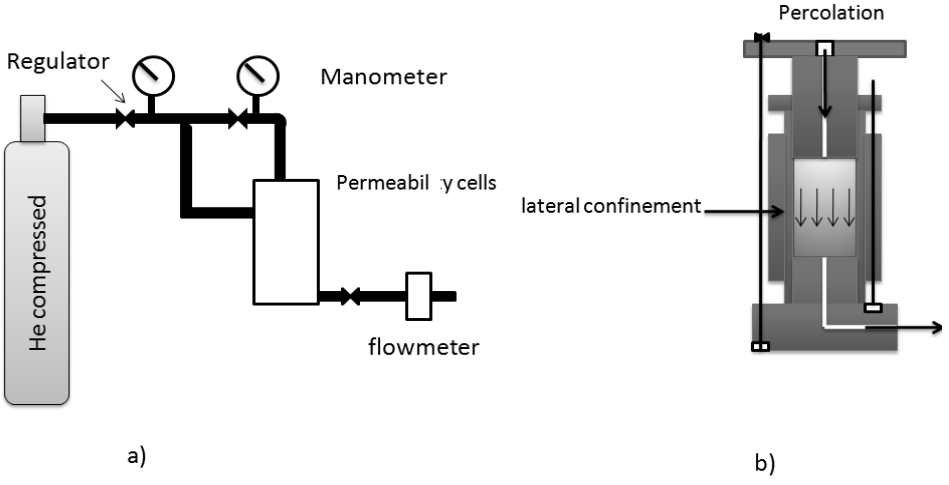

Figure 1: a) Representative diagram of the experimental device for measuring the permeability.
b) Permeability cell.

In this device, the cylindrical sample (Ø40 x h80 mm) is placed in the axial permeability cell in PVC. This cell allows injecting the percolation gas and ensuring the lateral sealing of the sample by the intermediary of a

rubber membrane wrapped by containment gas. A helium bottle from 20 MPa provided with an expander is used to deliver the percolation gas (up to 6 bars absolute pressure) and also the containment gas having a constant value of 9 bar absolute pressure. A vacuum pump is used for sample editing. The output of the cell is provided with a mass flow meter for measuring the released gas flow. The mass flowmeters of different capacity: 0-10 ml/min, 0-50 ml/min, 0- 200 ml/min, 0-500 ml/min are used, the mass flow depends on the sample output rate. A LabView data acquisition system was used to monitor the output flow with percolation time. The experimental principle of permeability determination is based on the measurement of the flow rate for a given pressure gradient. Subsequently, the gas apparent permeability is calculated from the overall flow of measured gaz passing through the sample by direct application of Darcy's law.

2.4. Compressive and flexural strength

The compressive and flexural tests were carried out on prismatic specimens 4x4x16cm as stated in the NF EN 196-1 [19]. Each specimen is first submitted to a bending test on 3 points. Then, the two half-pieces are tested in compression until failure. The compressive strength of a formulation is the arithmetic average of the four individual results obtained from four determinations on a set of two prisms. If a result among the four varies by more than ± 10% from the average, this result is removed and the arithmetic average is calculated from results of the remaining three. If a result of the three varies by more than ± 10% from their average, the overall results are rejected.

2.5. Scanning Electron Microscopy

The analyzes were performed on the SEM scanning electron microscopy field effect brand Jeol JSM6301F for observing dry samples was used for this study. To prepare the samples, simply drop the sample on a carbon scotch double sided. The samples are rendered conductive by carbon metallization before being observed by SEM.

3. Results and discussion

3.1. Apparent density

Figure 2 shows the evolution of the density of the mortar specimens after 28 days of curing in water at 20 °C, depending on the content of the binder additions treated. Each value in this figure is the average of the results obtained on three specimens. We note a steady decline in the density with various additions: the reference specimen has density of 2145kg/m^3, we notice that the density decreased with the additions, this decline is certainly attributed to the presence of a higher porosity in the specimen. These results are explained by the fact that the practical specifique surface area of the treated additions is greater than that of the cement, which can have a good influence on the mortars lightness. However, should be adding more water to the mortar if we have the same fluidity as the reference mortar. In fact, we set the W/C ratio equal to 0.5, consequently the mortar fluidity decreases depending on the rate of addition.

3.2 Porosity accessible to water

The porosity accessible to water is a parameter closely related to the material durability that quantifies the relative void volume but not its connectivity [20]. Figure 3 shows the evolution of the porosity accessible to water of samples after 28 days of curing in water depending on the content of additions to the binder. These are the same samples we used to determine the density. It is observed that the porosity evolves inversely with the density. We note from this study that the cement partial substitution by the shell powder and the nanocomposite in mortars causes an increase of the porosity accessible to water and at the same time, a decrease of the bulk density. The porosity accessible to water is a very important parameter when interpreting durability studies such as resistance to freeze/thaw and accelerated carbonation [21].

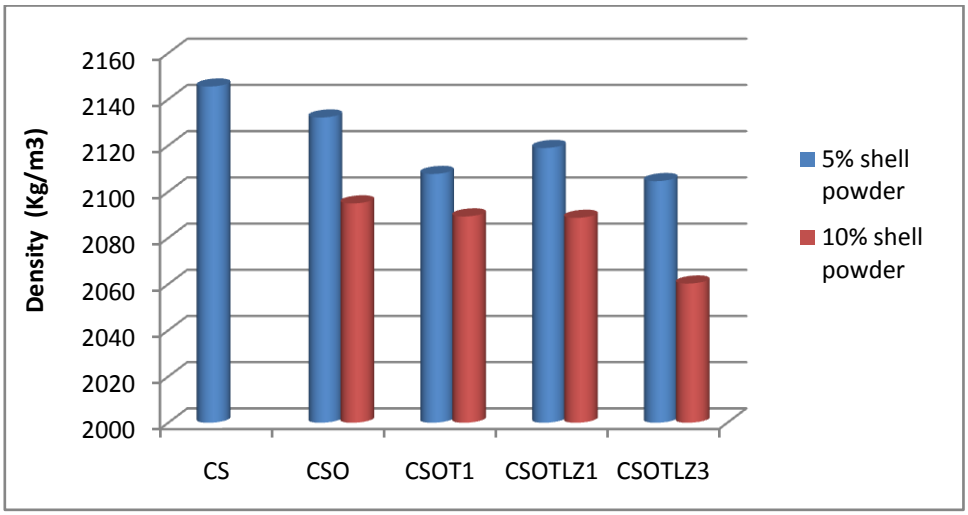

Figure 2: Apparent density of specimens after 28 days of curing in water.

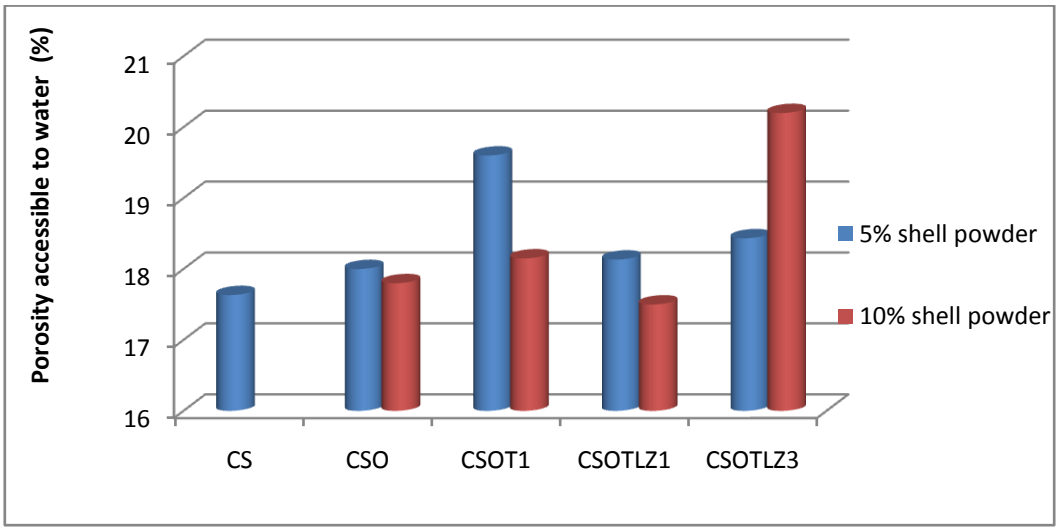

Figure 3: Porosity accessible to water of specimens after 28 days of curing in water.

3.3. Apparent permeability

The measurement results are shown in Figure 4. Each value is the average of measurements performed on three specimens. The main findings are:

- All mortars studied have a relatively low permeability of about 10^{-18} m^2 to 10^{-17} m^2. These values are comparable to that of an ordinary concrete observed by Picandet [22].
- Except CSOTLZ3 mortar with 5% shell powder, the mortars containing the additions have higher permeability than or equal to that of the reference mortar. This result is in accordance with the porosity increased observed by the previous measurements.
- The greatest value of permeability was observed for the sample CSOT1 with 5% shell powder.

These results show that the introduction of the shell powder and the nanocomposite powder in the mortars by substitution of the cement does not affect the permeability. Although the mortars containing these additions have porosities accessible to water upper than the reference mortar permeability remains almost the same order of magnitude. We can deduce that these porosities exist locally, and that the introduction of these additions does not increase the connectivity of these porosities. Somehow, this is a positive effect for the material durability [21].

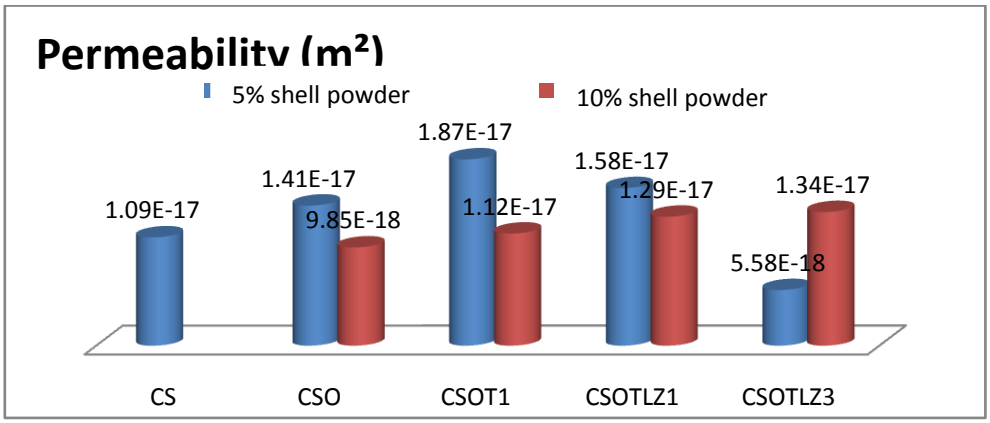

Figure 4: Specimens permeability of 28 days curing in water.

3.4. Compressive and flexural strength

The compressive strength is an important criterion to characterize the success of valuation and define the class of binder resistance. Figure 5 shows the evolution of resistances to 28 days depending on the additions percentage in the binder. We observe that the replacement of a portion of CEM I by additions leads to a small decrease in the compressive strength. These results are not surprising since the added nanocomposites do not have the same performance as Portland cement CEM I. The results show that the compressive strengths of mortars containing 10% of shell powder, except mortar CSO, are significantly higher than those of mortars with 5% shell powder. This result is comparable to that observed by Chaid A. et al. [23] on the increase of the limestone percentage which is responsible for the mechanical evolution; the limestones favorably affect the mechanical properties of concretes. In addition to their role granular causing increased compactness and consequently higher strength. According to Husson [24], they can have an accelerating effect and contribute to the formation of hydrated species due to their interaction with the tricalcium silicate phase of cement.

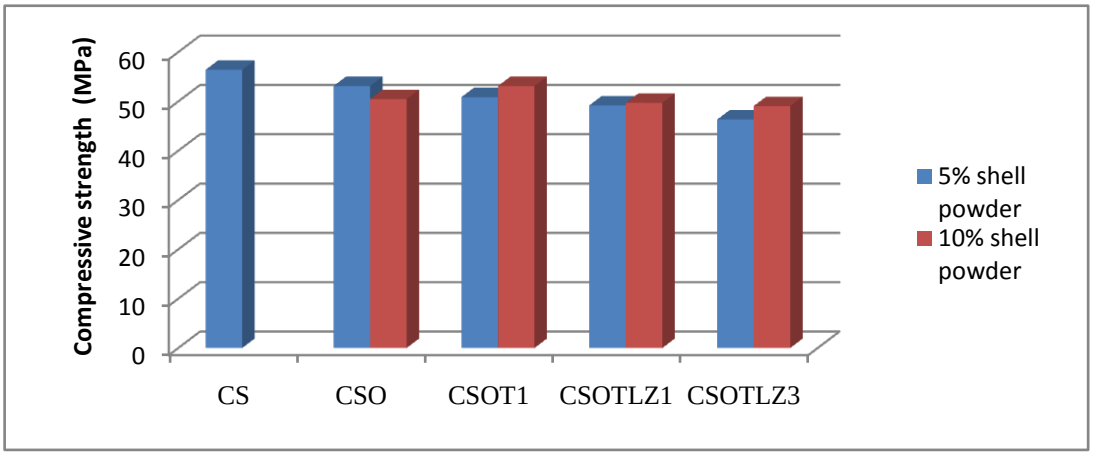

Figure 5: Compression strength of specimens (Ø4xh8 cm) after 28 days of curing in water.

The development of flexural strength for the different types of mortars kept in water is given in Figure 6. The flexural strength decreased for all mortars except mixtures CSOTLZ1 and CSO with 5% shell powder. The most important resistance observed corresponds to mortar CSOTLZ1 with 5% shell powder. These results are relatively in accordance to the compressive strength results. Indeed, in our study, the differences of behavior depending on the nature of the additions in the formulations are consistent with the results of the flexural and compressive strength. The CSOTLZ3 mortar that shows the low value of strengths also presents the higher value of the porosity accessible to water.

According to S. Assié [25], the first characteristic that should be represented as a function of the mechanical strength is the porosity accessible to water. This parameter is directly related to the mechanical strength of concrete [26].

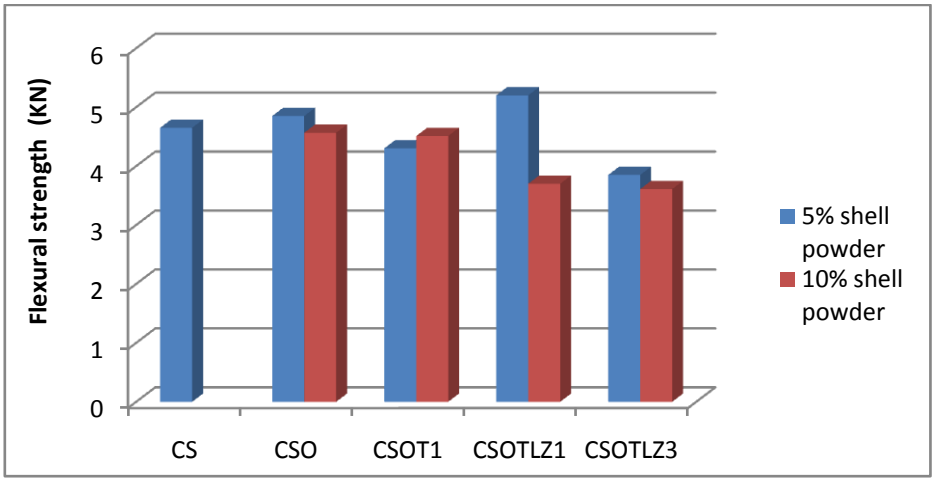

Figure 6: Flexural strength of specimens (Ø4xh8 cm) after 28 days of curing in water.

3.5. Scanning Electron Microscopy

Observations with a scanning electron microscope reveal the morphology of common components mortars (C-S-H, ettringite,...), and provide an explanation of changes in the pore structure of mortar: the formation of C-S-H and ettringite fills the pores between grains and between hydrates already formed (especially larger pores). The choice of illustrated micrographs is focused on the sample with 10% shell powder addition because of the obtained optimal results due to the relatively high amounts of addition.

The micrographs of Figure 7 of reference mortar (a) show the presence of portlandite plates surrounded by the cement paste (C-S-H + ettringite).

It is clearly noticed that the additions (TiO_2, shell powder and LDH-Zn-TiO_2 nanocomposite) acting on the specimens, giving rise to "C-S-H" very significantly altered appearance (b) and (c). Mortars with shell powder have a matching morphology consisting of large particles prismatic which increased the porosity. We also note that the sample CSO10T1 has more pores than other samples and the mortar CS is less porous which is confirmed in previous results of porosity. The presence of large pores may be due to a poor cohesion between the binder and the aggregate, probably because of the morphology of limestone disparate particles. This morphology limestone particles acting as fibers can facilitate the formation of a reinforced frame, wherein the smallest needles of calcium silicate hydrates could fill the spaces between the aggregate particles. These results are in agreement with the results of P. Ballester [27].

Conclusion

The study enabled the behavior evaluation of nanocomposites and shell powder additions in the cementitious matrix. The results show that the introduction of additions in the mortar does not affect significantly the permeability of the mortar. However, these additions are responsible for the increase of the porosity accessible to water and contribute to the reduction of the bulk density. The partial replacement of cement CEM I 52.5 by the additions lead to an inconsiderable decrease of the compressive and flexural strengths of the mortar. Observations from the scanning electron microscope showed the presence of portlandite plates surrounded by the cement paste (CSH + ettringite). Mortars with shell powder have a different morphology as large prismatic particles, which results in the appearance of more pores. In sum, these results show a real feasibility of using additions; nanocomposites, shell powder; probably for specific applications of cement based materials.

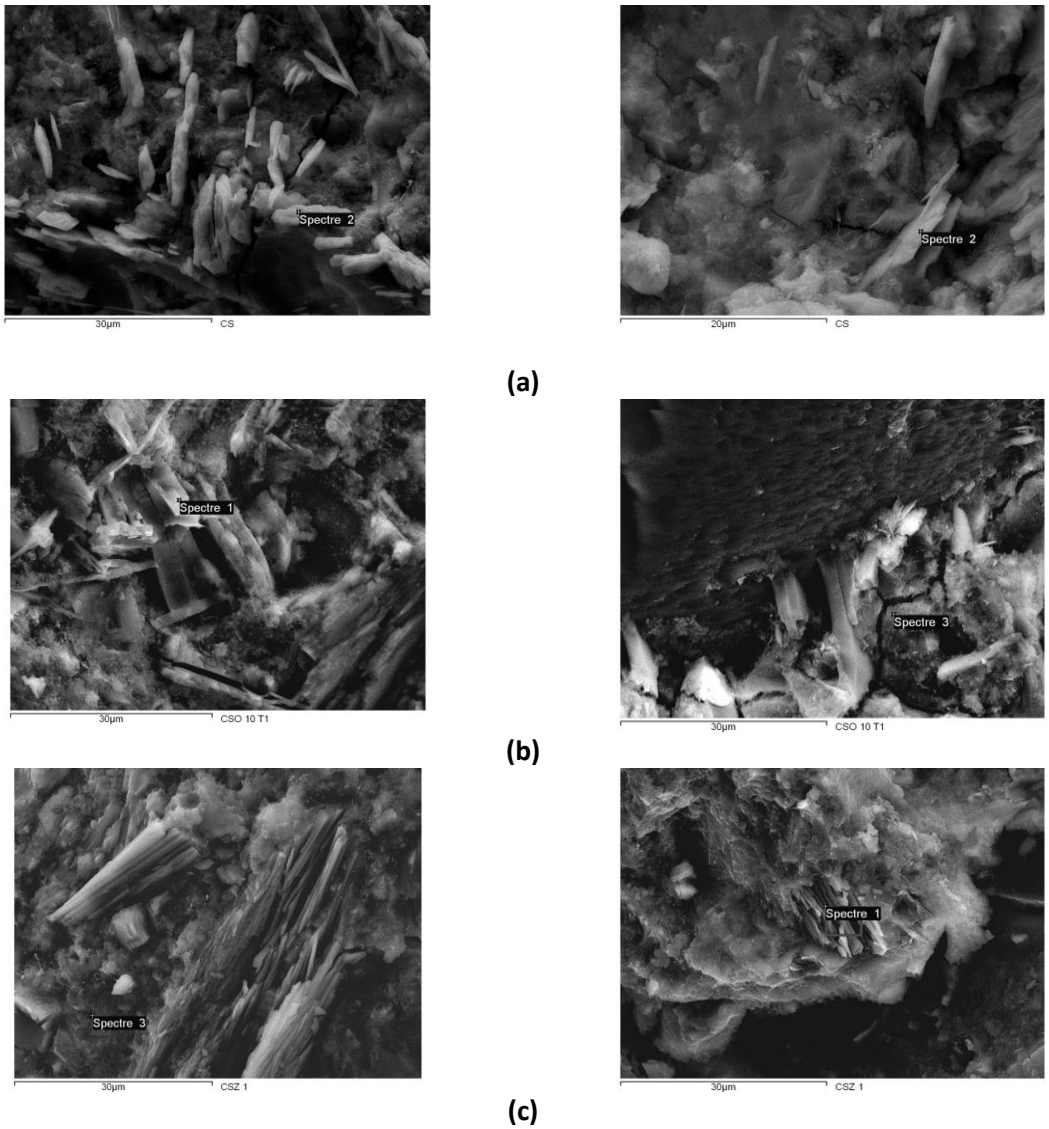

Figure 7: SEM micrographs of mortars after 28 days of hydration (a) CS (b) CSO10T1 (c) CSO10TLZ1.

Acknowledgement-The authors would like to thank Huber Curient Volubilis Program for the financial support given by the grant N° MA/10/236 in the framework of a France- Morocco exchange.

References

1. Chen J, Poon CS., *Environ Sci. Technol*. 43(2009) 52.
2. Chen J, Kou SC, Poon CS., *Build Environ*. 46(2011) 33.
3. B, Plassais A, Olive F, Guillot L, Bonafous L., *Sol. Energ*. 83 (2009) 801.
4. Augugliario V, Loddo V, Pagliaro M, Palmisano G, Palmisano L., *R.S.C. J*. 978 (2010) 870.
5. Aissa AH, Puzenatm E, Plassais A, Herrmann JM, Haehnel C, Guillard C., *Appl. Catal. B. Environ.* 1 (2011) 8.
6. Diamanti MV, Ormellese M, Pedeferri M., *Cem. Concr. Res.* 38 (2008) 53.
7. Nazari A, Riahi S., *Energ. Build.* 995 (2011) 1002.
8. Sanchez F, Sobolov K., *Constr. Build. Mater*. 2060 (2010) 71.
9. Potgieter J.H., Horne K.A., Potgieter S., Wirth W., *Mater. Lett*. 157 (2002) 163.
10. Martinez T., Escadeillas G. Revêtements photocatalytiques pour matériaux de construction : formulation, évaluation de l'efficacité et écotoxicité. *Thèse de doctorat*, Univ. Toulouse III, (2012).

11. Jargot D., La Rocca B., Malard S. *Fiche toxicologique*, Dioxyde de titane, INRS, (2013).
12. Zhang MH, Li H., *Constr. Buil. Mater*. 608 (2011) 616.
13. Treadewell, Bernasconi E., *Helvetica Chim. Acta.* 500 (1930) 509.
14. Feitknecht W., *Helvetica Chim. Acta.* 766 (1938) 784.
15. Vulic T., Hadnadjev-Kostic M., Rudic O., Radeka M., Marinkovic-Neducin R., Ranogajec J., *Cem. Concr. Compos.* 121 (2013) 127.
16. Zamorani E., Sheik I., Serrini G., *Cem. Concr. Res*. 259 (1989) 266.
17. Yip C.K., Provis John L., Lukey Grant C., Van Deventer J.S.J., *Cem. Concr. Compos.* 30 (2008) 979–985.
18. *AFREM Group* : Les résultats des essais croisés AFREM pour la détermination de la masse volumique apparente et de la porosité accessible à l'eau des bétons.
19. *NF EN 196-1*. Indice de classement P 15-471-1, Avril (2006).
20. Hermida G. Influence du volume de pâte et de la concentration en ciment sur la performance du béton : vers le développement d'un béton à contenu minimal en pâte. *Thèse de doctorat*. Ecole normale supérieure de Cachan, (2008).
21. Dang T. A., Valorisation des sédiments marins bretons comme matériaux de construction. *Thèse doc*. , INSA Rennes, (2011).
22. Picandet V. Influence d'un endommagement mécanique sur la perméabilité et sur la diffusivité hydrique des bétons. *Thèse de doctorat*. Ecole doctorale mécanique, thermique et génie civil de Nantes, (2001).
23. Chaid R., Jauberthie R., Boukhaled A., *Leban. Sci. J.* 91 (2010) 103.
24. Husson S. Etude physicochimique et mécanique des interactions ciment-filler, Application aux mortiers. *Thèse doctorat*, INIST-CNRS, Cote INIST : T 82906, (1991).
25. Assié S. Durabilité des bétons autoplaçant. *Thèse de doctorat*, INSA Toulouse, (2004).
26. Bessa A,. Bigas J.P,. Gallias J-L. Evaluation de la contribution liante des additions minérales à la porosité, à la résistance en compression et à la durabilité des mortiers. *XXIIIème Rencontres Universitaires de Génie Civil*, Ville & Génie Civil. L'université Marne-la-Vallée France, (2004).
27. Ballester P., Mármol I., Morales J., Sánchez L., *Cem. Concr. Res.* 559 (2007) 564.
28. Fatimah Is., *J. Mater. Environ. Sci.* 983 (2012) 992.
29. Sakthivel S., Neppolian B., Shankar MV., Arabindoo B., Palanichamy M., Murugesan V., *Sol. Energ. Mat. Sol. Cells*. 65 (2003) 82.
30. Yoon G.L., Kim B.T., Kim B.O., Han S.H., *Waste Manage*., 825 (2003) 834.
31. Wang H.Y., Kuo WT., Lin CC., Chen PY. *Constr. Build. Mater*. 41, 532 (2013) 537.
32. Yang E.I., Yi S.T., Leem Y.M., *Cem. Concr. Res*. 2175 (2005) 2182.